Developing and Validating a Multivariable Prediction Model to Improve the Diagnostic Accuracy in Determination of Cervical versus Endometrial Origin of Uterine Adenocarcinomas: A Prospective MR Study Combining Diffusion-Weighted Imaging and Spectroscopy

Gigin Lin, MD, PhD [ID],[1,2,3†] Yu-Chun Lin, PhD,[1,2†] Ren-Chin Wu, MD, PhD,[4]
Lan-Yan Yang, PhD,[5,6] Hsin-Ying Lu, MSc,[1,2,3] Shang-Yueh Tsai, PhD,[7]
Yu-Ting Huang, MD,[8] Yen-Ling Huang, MD,[1] Kuan-Ying Lu, MSc,[1,2,3]
Koon-Kwan Ng, MD,[8] Tzu-Chen Yen, MD, PhD,[9] Angel Chao, MD, PhD,[5,6]
Chyong-Huey Lai, MD,[5,6] and Ji-Hong Hong, MD, PhD[2,10]

Background: A triage test to assist clinical decision-making on choosing primary chemoradiation for cervical carcinomas or primary surgery for endometrial carcinomas is important.

Purpose or Hypothesis: To develop and validate a multiparametric prediction model based on MR imaging and spectroscopy in distinguishing adenocarcinomas of uterine cervical or endometrial origin.

Study Type: Prospective diagnostic accuracy study.

Population: Eighty-seven women: 25 cervical and 62 endometrial adenocarcinomas divided into training (n = 43; cervical/endometrial adenocarcinomas = 11/32) and validation (n = 44; 14/30) datasets.

Field Strength/Sequence: The 3T diffusion-weighted (DW) MR imaging and MR spectroscopy.

Assessment: Morphology, volumetric DW MR imaging and spectroscopy (MDS) scoring system with total points 0–5, based on presence of the following MR features assessed independently by two radiologists: (a) epicenter at the cervix, (b) rim enhancement, (c) disrupted cervical stromal integrity, (d) mean volumetric apparent diffusion coefficient values (ADCmean) higher than $0.98 \times 10\text{-}3 \, \text{mm}^2/\text{s}$, (e) fatty acyl δ 1.3 ppm more than 161.92 mM. Histopathology as gold standard.

Statistical Tests: Logistic regression and receiver operator characteristic (ROC) curves analysis.

Results: For both the training and validation datasets, the MDS score achieved an accuracy of 93.0% and 84.1%, significantly higher than that of morphology (88.4% and 79.5%), ADC value (74.4% and 68.2%), and spectroscopy (81.4% and 68.2%; $P < 0.05$ for all). The performances of the scoring were superior to the morphology in the training dataset (areas under the receiver operating characteristics curve [AUC] = 0.95 vs. 0.89; $P = 0.046$), but not in the validation dataset (AUC = 0.90 vs. 0.85; $P = 0.289$).
Data Conclusion: MDS score has potentials to improve distinguishing adenocarcinomas of cervical or endometrial origin, and warrants large-scale studies for further validation.
Level of Evidence: 1
Technical Efficacy: Stage 3

Endometrial and cervical carcinomas are common malignancies in the female pelvis in the United States.[1] Differentiating the tumor origin from cervix or endometrium is crucial for treatment selection based on the National Comprehensive Cancer Network (NCCN) guideline.[2] Primary surgery is the recommended treatment for all stages endometrial carcinoma. In cervical carcinomas, radical hysterectomy with pelvic lymphadenectomy is the preferred option for stage IB1-IIA1 disease, while stage IIB or above primarily being treated with chemoradiation.[3] Not infrequently, clinicians might encounter difficulties in distinguishing the origin of tumors solely based on the biopsy specimens because of inadequate samples, absence of precursor lesions, mixed histologic types, unusual morphologic patterns or poorly differentiated tumors.[4] In such situation, the use of immunohistochemical (IHC) panels has found to be useful.[4] Adenocarcinomas originated from endometrium are characterized by positive staining for vimentin and estrogen receptors (ER),[5] whereas adenocarcinomas originate from the cervix demonstrating the positivity of carcinoembryonic antigen (CEA)[5] and p16, a surrogate for the presence of human papillomavirus infection.[6] Because no single antibody is entirely specific for cervical or endometrial carcinomas, more imaging information would be helpful for pathologists when the sampled tissue is limited.

Magnetic resonance (MR) imaging the standard of care for the assessment of the clinical stage and disease extent of cervix or endometrium carcinomas.[7] Conventional MR imaging based on morphological findings shows utility in determining anatomical tumor origins,[8–10] but the observations are subjective.[11] With the advancement of MR technologies, the diffusion-weighted (DW) MR imaging has emerged as a useful tool to evaluate myometrial invasion depth of endometrial cancer,[12,13] and depict endometrial cancers with cervical stromal invasion.[14] Apparent diffusion coefficient (ADC) values on DW MR imaging is based on the information about water mobility which reflecting the tissue cellularity and the membrane integrity.[13] Preliminary reports have shown the ADC values derived from a single slice section of DW MR imaging might help in determining the origins from cervix or endometrium,[15] which yet to be validated in a more rigorous volumetric ADC histogram analysis of the whole tumor. Additionally, MR spectroscopy using external phase array coils at 3.0T provides measurements of tumor biochemistry in vivo for patients with cervical cancer.[16] It remains unknown whether the integration of quantitative DW MR imaging and MR spectroscopy into the conventional morphological observations will improve the diagnosis of tumor origins from cervix or endometrium.

The aim of this study is to develop and validate a multiparametric prediction model based on morphology, DW MR imaging, and MR spectroscopy, in distinguishing adenocarcinomas of cervical or endometrial origins.

Materials and Methods

Participants Patients

This study complied with the Transparent Reporting of a Multivariable Prediction Model for Individual Prognosis or Diagnosis, or TRIPOD Statement.[17] The institutional review board approved the protocol of this prospective diagnostic accuracy study (NCT01874548 and NCT02528864), and informed consents were obtained in a tertiary referral center with a dedicated gynecology oncology interdisciplinary team to screen patient enrollment. From July 2013 to April 2017, we screened a consecutive cohort of 283 patients. Inclusion criteria included (1) female age 20–80, (2) clinical suspicion of cervical or endometrial malignancy for pretreatment staging. Exclusion criteria included (1) contraindications to MR scanning, such as claustrophobia, cardiac pacemaker, metal implants in the field of views. Impaired renal function with estimated glomerular filtration rates less than $60 \, mL/min/1.73 \, m^2$ or unable to cooperate for MR study due to mental status, (2) lesion size $< 1.5 \, cm$, (3) suboptimal MR imaging quality. We filtered the patients with tumors locating at the low uterine segment or cervix, and pathology review yielded adeno- or adenosquamous carcinomas for this report. The flow diagram of study cohort is detailed in Figure 1. Thirteen cases of the study cohort has been previously reported to investigate the clinical values of proton MR spectroscopy in prediction of poor prognostic human papillomavirus (HPV) genotypes.[16]

MR Methods

MR Studies were conducted with a 3T MR imaging unit (Skyra, Siemens, Erlangen, Germany) before treatment. We used the integrated spine coil and the body-phased array coil to cover the entire pelvis in the supine position.[16] Details of MR acquisition protocols for morphological T1-weighted, T2-weighted, and DW MR imaging (b = 0, 1000 s/mm²) are listed in Table 1. DCE MR imaging was performed at 0, 45, 90, 180 s with an intravenous bolus injection of 0.1 mmol/kg body weight of contrast medium
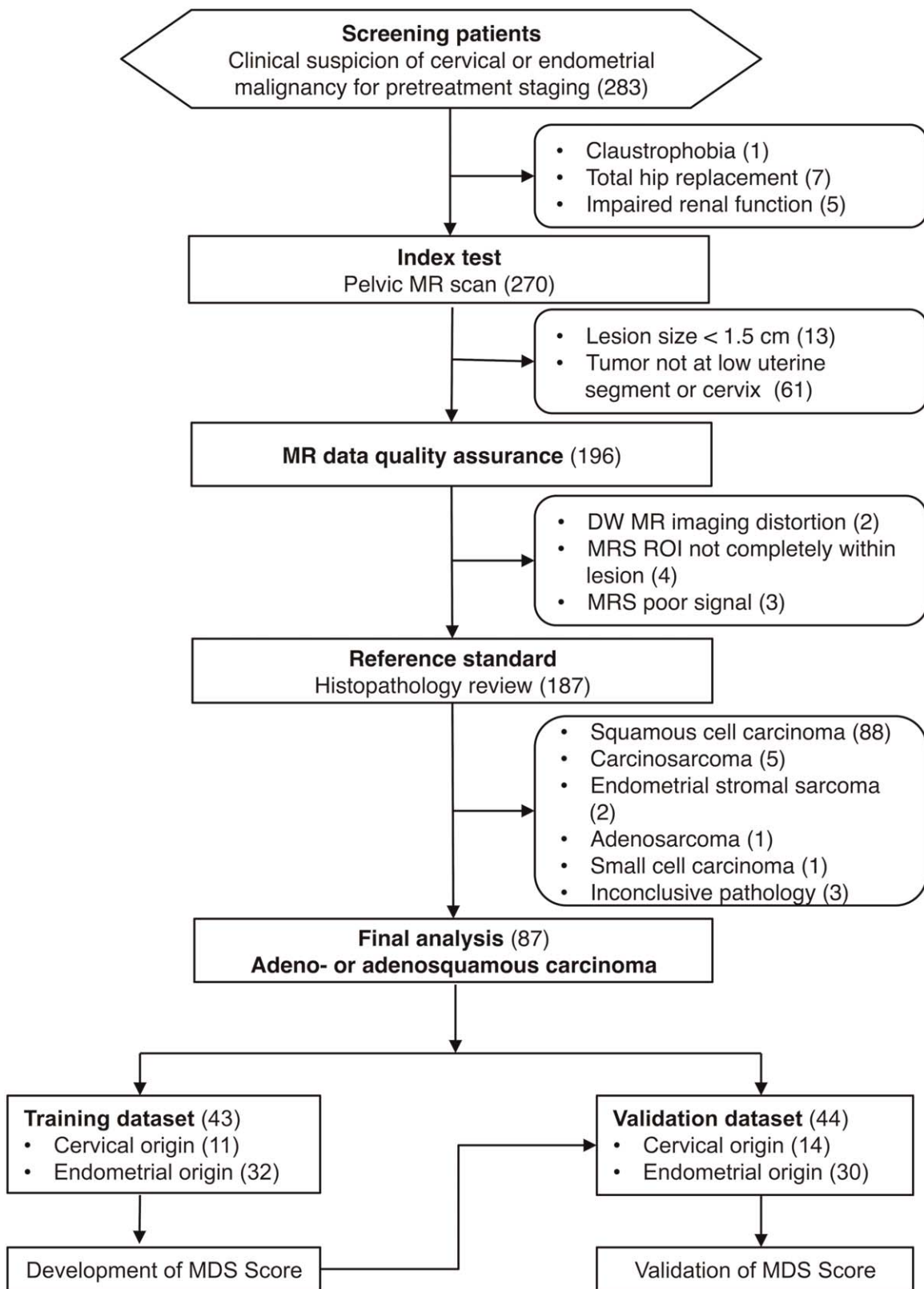
FIGURE 1: Flow diagram of study cohort.

(gadopentetate dimeglumine, Magnevist, Schering, Berlin, Germany) followed by a 20-mL saline flush with an injection rate of 3 mL/s. This study was performed during minimal breathing. No premedication was administered.

MR Spectroscopy

We used triplane localizer 1D MR spectroscopy with point-resolved spectroscopy (PRESS), with the volume of interest (VOI) $12 \times 12 \times 12$ mm^3 prescribed by gynecological radiologists (G.L.

TABLE 1. Acquisition Protocol

	DCE-MR imaging	DW imaging	T2W imaging	T1W imaging
Pulse sequence	Turbo spin echo	Single-shot echo-planar	Turbo spin echo	Turbo spin echo
Orientation	Axial and sagittal	Axial and sagittal	Axial and sagittal	Axial
Slice thickness/Gap (mm)	4/1	4/1	4/1	4/1
Repetition time (ms)	567	3300	5630	626
Echo time (ms)	10	79	87	11
Field of view (cm)	20	30	20	20
Acquisition matrix (phase × frequency)	256 × 320	128 × 128	256 × 320	256 × 320
Averages (NEX)	2	4 (both b-0 and b-1000)	3	2
Echo train length (ETL)	5	120	13	3
Flip angle	150	180	150	150
GRAPPA factor	2	2	2	2
Fat saturation	CHESS	CHESS	None	None
Acquisition time (s)	185	63	176	133

CE-MR = contrast enhanced MR; CHESS = chemically selective suppression; DWI = diffusion-weighted (b = 0, 1000 s/mm^2); GRAPPA = generalized auto-calibrating partially parallel acquisition; T1W = T1-weighted; T2W = T2-weighted; NEX = number of excitations.

or Y.T.H.), completely placed within the mass. We optimized the following parameters for PRESS: TR/TE, 2000 ms/35 ms; 128 averages; vector size, 1024 points; bandwidth, 1200 Hz; water suppression, selective band inversion with gradient dephasing; non-water suppressed spectra as concentration references, four averages. The total MR scanning time including spectroscopy was within 45 min.

Imaging Predictors

MORPHOLOGY. Two radiologists with 12 (G.L.) and 9 (Y.T.H.) years' experience in gynecological radiology interpreted MR images independently blinded to clinical and histological information. The consensus was made for final analysis. The definitions of morphology traits are detailed in Table 2.

ADC VALUE. The ADC maps were generated using a monoexponential decay model (VD17; Siemens). The volumetric ADC data were collected by manually delineating the regions of tumor on sagittal ADC maps slice-by-slice through the whole tumor for each patient, using in-house developed software based on Matlab (Mathworks, Natick, MA). The first radiologist drew regions of interest (ROIs) around the tumor on each section on the ADC maps with reference to the high b-value DW images to delineate the whole tumor volume to minimize the slice selection bias. The second radiologist independently verified the ROIs. The histogram parameters of the volumetric ADC data were extracted: the mean, minimum, 10th, 25th, 50th, 75th, and 90th percentiles and maximal pixel ADC values (ADCmean, ADCmin, ADC10, ADC25, ADC50, ADC75, ADC90, and ADCmax, respectively).

MR SPECTROSCOPY. Data were analyzed using the LCModel software (version 6.3–0 K; Provencher, Ontario, CA, Canada) on a

TABLE 2. Definitions of Morphological Imaging Traits

| Trait	Description	References
Cervical location	Locations of the epicenter at cervical canal	8-10, 18
Hypervascular perfusion	Tumor enhancement higher than that of normal myometrium at the arterial phase of DCE-MR imaging ☐	8, 18, 19
Rim enhancement	Complete or incomplete enhancement on DCE-MR imaging at the periphery of the tumor ☐	18
Absence of deep myometrial invasion	The ratio of the deepest outer tumor margin over total myometrial thickness not exceeding 50%	10, 18
Disruption of cervical stromal integrity	Disruption of cervical stromal integrity	18
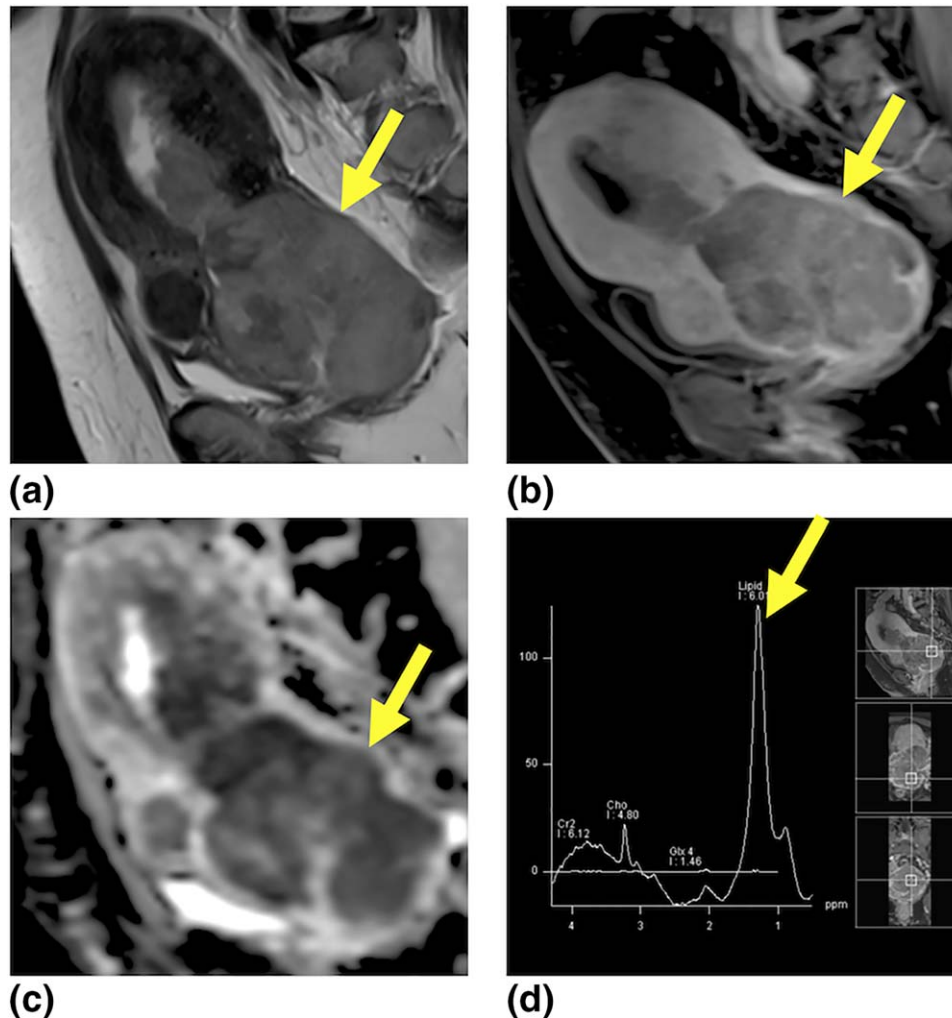
FIGURE 2: Cervical adenocarcinoma (arrow) in a 49-year-old woman. Sagittal T2-weighted (TR/TE 5630/87) (a), postcontrast T1-weighted image (80/3) after intravenous gadolinium contrast administration at 120 s (b), fused T2-weighted and DW MR images (c), MR spectroscopy (d). Tumor epicenter at cervix (*yes*), presence of rim enhancement (*yes*) and disrupted cervical stromal integrity (*yes*), $ADC_{mean} = 1.13 \times 10^{-3}$ mm^2/s, lipid δ 1.3 ppm = 699.32 mM. MDS score = 5. The final histopathology yielded to be a cervical adenocarcinoma (Grade 3).

Linux workstation, which applied a linear combination of multiple spectra defined on the "Tumor" basis, by generating a Gaussian peak between a minimum and expected linewidth for each simulated peak, then applying a Lorentzian line-broadening to them all (LCModel User's Manual). The resonances were quantified relative to the water signal. The Cramer-Rao lower bound (CRLB) value, which simultaneously accounts for both line width and signal-to-noise ratio, was calculated as an estimate of the error in metabolite quantification. MR spectra were excluded if the CRLB exceeded 20% for creatine (δ 3.0 and 3.9 ppm), choline (δ 3.2 ppm), myo-Inositol (δ 3.5 ppm), lipid methyl (δ 0.9 ppm), and lipid methylene (δ 1.3 ppm), and 30% for Glx (δ 2.2–2.4 ppm), lipid unsaturated (δ 2.0 ppm).

Histopathology Outcome

The reference standard was based on the histopathology obtained from surgical specimens during standard operations (n = 79) or punch biopsy (n = 8). If the primary site of the tumor was uncertain, an additional immunohistochemical study was performed to confirm the adeno-/adenosquamous carcinomas of cervical or endometrial origins. The consensus of a general pathologist and a specialized gynecological pathologist (R.C.W.) confirmed the histopathologic types and tumor differentiations, with the clinical information and morphologic MR imaging reports available.

Statistical Analysis

The data were analyzed using MedCalc for Windows, Version 9.2.0.0 (MedCalc Software, Mariakerke, Belgium), or R Package for Statistical Computing (www.r-project.org). The study sample size arrived at the continuous prospective cohort. A total of 87 patients were eligible for final analysis, including 25 cervical and 62 endometrial adenocarcinomas divided into training (n = 43; cervical/endometrial adenocarcinomas = 11/32) and validation (n = 44; 14/30) datasets. Using univariate and stepwise multivariate regression and Wald test, we developed a morphology, volumetric DW MR imaging and spectroscopy (MDS) score from the training dataset (n = 43; July 2013 to June 2015). Representative cases are presented as Figures 2 and 3. We used complete-case analysis, and nine missing data were excluded from final analysis. We internally validated the Training dataset by bootstrap resampling
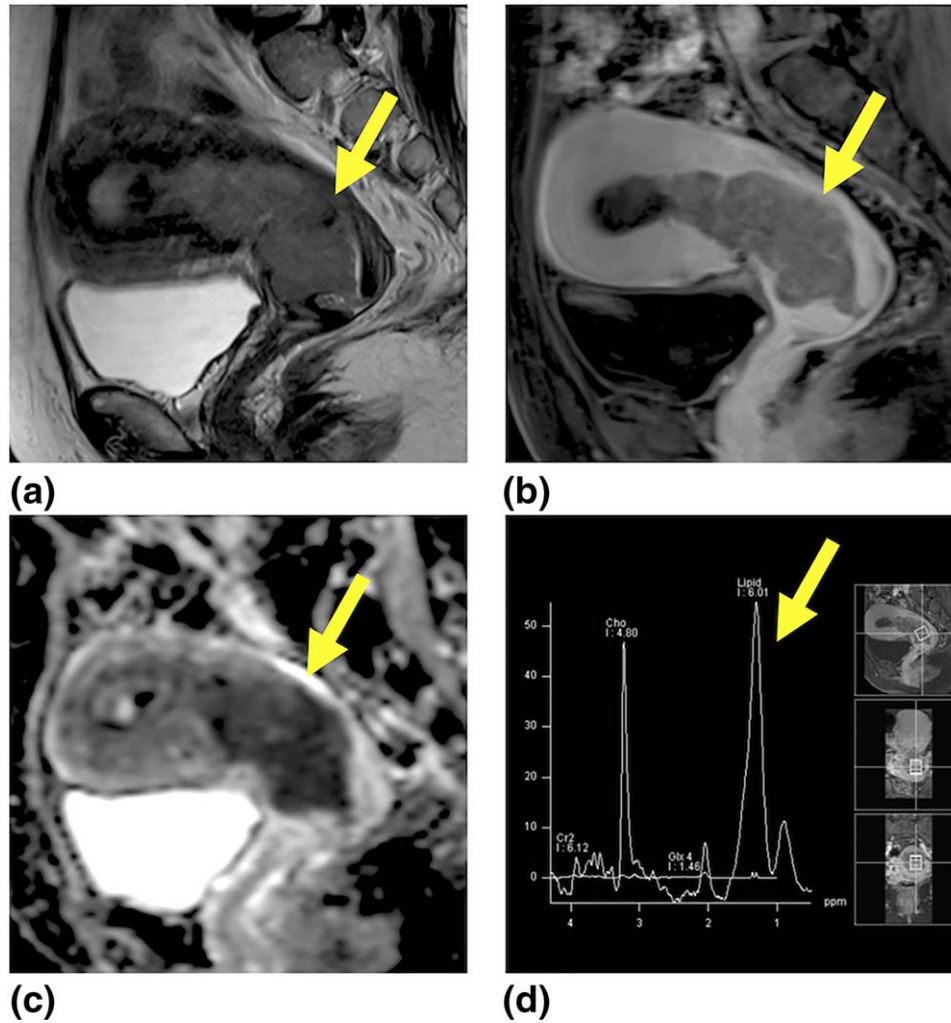
FIGURE 3: Endometrial carcinoma (arrow) in a 52-year-old woman. Sagittal T2-weighted (TR/TE 5630/87) (a), postcontrast T1-weighted image (80/3) after intravenous gadolinium contrast administration at 120 s (b), fused T2-weighted and DW MR images (c), and MR spectroscopy (d). Tumor epicenter at cervix (*yes*), presence of rim enhancement (*no*) and disrupted cervical stromal integrity (*yes*), $ADC_{mean} = 0.67 \times 10^{-3}$ mm^2/s, lipid δ 1.3 ppm = 118.91 mM). MDS score = 2. The final histopathology yielded to be an endometrial adenocarcinoma (endometrioid type; Grade 3).

randomly to construct new data sets followed by logistic regression analysis repeated for 1000 times, to prevent data overfitting. The predictive values of MDS score were validated independently (n = 44; July 2015 to April 2017). The cutoff values of ADC values and MR spectroscopy were determined by using receiver operating characteristics (ROC) analysis. The validation data were the same as the training data regarding setting, eligibility criteria, outcome, and predictors (Table 3).

Reader agreements on imaging traits were analyzed using weighted kappa statistics ($0.00 \leq \kappa < 0.40$, poor; $0.40 \leq \kappa \leq 0.70$, moderate; $0.70 \leq \kappa \leq 0.90$, good; $\kappa > 0.90$, excellent). The overall sensitivity, specificity, and diagnostic accuracy of using morphology, ADC values, MR spectroscopy, and the MDS score, were determined based on the histopathological reference of were represented with 95% confidence intervals (CIs), using McNemar test to compare between groups. We selected significant univariate predictors in the training dataset to carry forward to four models (morphology, ADC values, MR spectroscopy, and the MDS score) designed to test the incremental benefit of groups of predictors, and areas

under the receiver operating characteristics curve (AUC) were calculated to compare diagnostic performance among models. No model updating or recalibration was raised from the validation. $P < 0.05$ was considered to indicate a significant difference.

Results

Patient Cohort

A total of 87 patients were eligible for final analysis; age ranged from 34 to 80 years (median, 59 years). Figure 1 demonstrates the flow diagram of the study cohort. The cervical and endometrial cancer patients demonstrated no statistically significant differences in the clinical and demographic characteristics (Table 3). Time interval and any clinical interventions between MR study and histopathology were 1–30 days (median, 13 days). No adverse events from performing the MR study. The reader agreements of morphologic imaging trait were excellent for

TABLE 3. Patient Demographics and Histopathology Characteristics[a]

| Variable | Cervix (n = 25) | | Endometrium (n = 62) | | P-Value[c] |
	Training	Validation	Training	Validation	
n,	11	14	32	30	
Age, median (y)[b]	52 (34-63)	54 (42-79)	53 (39-71)	53 (35-83)	0.637
Weight, median (kg)[b]	60 (44-75)	58 (42-77)	61 (41-89)	59 (45-94)	0.649
Tumor size, median (cm)[b]	4 (1-5)	4 (1-6)	5 (2-10)	4 (2-11)	0.802
Histopathology					0.266
Adenocarcinoma	7 (64)	12 (86)	31 (97)	30 (100)	
Adenosquamous carcinoma	4 (36)	2 (14)	1 (3)	0 (0)	
Differentiation					0.740
Well	2 (18)	3 (21)	11 (34)	7 (23)	
Moderate	3 (27)	7 (50)	12 (38)	11 (37)	
Poor	6 (55)	4 (29)	9 (28)	12 (40)	
T stage					1.000
1, 2	10 (91)	13 (93)	31 (97)	28 (93)	
3, 4	1 (9)	1 (7)	1 (3)	2 (7)	
N stage					0.383
0	9 (82)	10 (71)	29 (91)	25 (83)	
1	2 (18)	4 (29)	3 (9)	5 (17)	
M stage					1.000
0	10 (91)	11 (79)	31 (97)	30 (100)	
1	1 (9)	3 (21)	1 (3)	0 (0)	
SCC-Ag (ng/mL)	1 (0-8)	1 (0-2)	1 (1-3)	1 (1-5)	0.940
CEA (ng/mL)	2 (0-41)	2 (0-850)	1 (1-62)	1 (1-162)	0.141

[a]Data in parentheses are %.
[b]Median (range).
[c]Cervix (n = 25) vs. endometrium (n = 62).

cervical location ($\kappa = 0.976$) and absence of deep myometrial invasion ($\kappa = 0.972$), good for disruption of cervical stromal integrity ($\kappa = 0.791$) and rim enhancement ($\kappa = 0.702$), and moderate for hypervascular perfusion ($\kappa = 0.628$).

Univariate Logistic Regression on Training Dataset

Table 4 shows the logistic regression analysis of factors associated with adenocarcinoma of cervical origin in the training dataset. Tumor epicenter at the cervix ($P = 0.001$), presence of rim enhancement ($P = 0.016$), and disrupted cervical stromal integrity ($P = 0.001$) were the three outstanding morphology traits demonstrating the significant predictive values. ADC_{mean} was chosen from the significantly predictive ADC parameters of ADC_{mean} ($P = 0.016$), ADC_{10} ($P = 0.008$), ADC_{25} ($P = 0.009$), and ADC_{50} ($P = 0.009$). Fatty acyl δ 1.3 ppm was chosen from the significantly

predictive spectroscopy parameters of fatty acyls δ 0.9 ppm ($P = 0.027$), δ 1.3 ppm ($P = 0.001$), and δ 2.0 ppm ($P = 0.016$). The predictive value of total choline was borderline but not significant ($P = 0.058$). We constructed an MDS scoring system with total points 0–5, based on presence of the following MR features: (a) epicenter at the cervix, (b) rim enhancement, (c) disrupted cervical stromal integrity, (d) mean volumetric apparent diffusion coefficient values (ADC_{mean}) higher than 0.98×10^{-3} mm^2/s, (e) fatty acyl δ 1.3 ppm more than 161.92 mM.

Accuracy Tests on Training and Validation datasets

Table 5 demonstrates the diagnostic results in determining tumor origins from cervix or endometrium in the training and validation datasets. In the Training dataset, the MDS score achieved an accuracy of 93.0%, significantly higher

TABLE 4. Logistic Regression Analysis of Factors Associated with Adenocarcinoma of Cervical Origin in the Training Dataset[a]

Attribute	OR	95%	CI	P value
Morphology traits				
Tumor location	54.0	7.9	1114.5	0.001[b]
Hypervascular perfusion pattern	1.8	0.4	13.0	0.518
Rim enhancement	6.2	1.5	30.4	0.016
Retained endometrial secretion	3.0	0.7	13.1	0.141
Absence of deep myometrial invasion	3.1	0.7	22.4	0.191
Disrupted cervical stromal integrity	16.9	3.4	110.2	0.001
ADC values				
ADC_{mean} ($> 0.98 \times 10^{-3}$ mm^2/sec)	6.2	1.5	30.4	0.016
ADC_{min} ($> 0.56 \times 10^{-3}$ mm^2/sec)	3.6	0.8	16.5	0.089
ADC_{10} ($> 0.71 \times 10^{-3}$ mm^2/sec)	9.9	2.1	73.3	0.008[b]
ADC_{25} ($> 0.89 \times 10^{-3}$ mm^2/sec)	7.6	1.8	38.1	0.009
ADC_{50} ($> 0.98 \times 10^{-3}$ mm^2/sec)	7.6	1.8	38.1	0.009
ADC_{75} ($> 1.12 \times 10^{-3}$ mm^2/sec)	6.2	1.5	30.4	0.016
ADC_{90} ($> 1.21 \times 10^{-3}$ mm^2/sec)	5.9	1.4	31.4	0.023
ADC_{max} ($> 1.76 \times 10^{-3}$ mm^2/sec)	3.0	0.7	15.8	0.148
Spectroscopy				
Lipid methylene δ 1.3 ppm (> 161.92 mM)	14.4	3.1	86.7	0.001[b]
Lipid methyl δ 0.9 ppm (> 20.40 mM)	5.2	1.3	24.9	0.027
Lipid unsaturated δ 2.0 ppm (> 18.19 mM)	6.2	1.5	30.4	0.016
Total choline δ 3.2 ppm (< 4.29 mM)	5.1	1.1	37.1	0.058
Creatine δ 3.0 and 3.9 ppm (> 0.08 mM)	3.1	0.6	15.0	0.156
Glx δ 2.2-2.4 ppm (< 6.73 mM)	3.3	0.8	15.2	0.098
Myo-Inositol δ 3.5 ppm (< 1.92 mM)	3.1	0.7	13.3	0.121

[a]Odds ratio data are reported per 1-unit increase.
[b]Multivariate stepwise selection significant.
OR = odds ratio; Glx = glutamine + glutamate

than that of morphology (88.4%), ADC value (74.4%) and spectroscopy (81.4%), in the diagnosis of tumors from the cervical origin. A significant improvement in specificity was found by using the MDS score (96.9%), as compared with that of morphology (90.6%), ADC value (78.1%), and spectroscopy (84.6%). In the Validation dataset, the MDS score achieved an accuracy of 84.1%, significantly higher than that of morphology (79.5%), ADC value (68.2%), and spectroscopy (68.2%), respectively ($P < 0.05$ for all).

ROC Comparisons of Models
Figure 4 and Table 6 show the comparisons of ROC curves based on morphology, ADC value, MR spectroscopy and combinations for the training and validation datasets. The overall diagnostic performances of morphological MR imaging (AUC = 0.89) was significantly improved only in combining both the ADC value and spectroscopy (AUC = 0.95; $P = 0.046$), but not in combining ADC value (AUC = 0.93; $P = 0.320$) or spectroscopy alone (AUC = 0.91; $P = 0.245$). A similar trend of improvement of the combined score was observed in the validation dataset (AUC = 0.90), albeit not statistically significant.

ADC Values in Different Tumor Differentiations
The ADC_{mean} values of cervical carcinomas were significantly higher than that of endometrial carcinomas in the moderately differentiated (mean ± standard error of mean, 1.18 ± 0.1 vs. $0.91 \pm 0.0 \times 10^{-3}$ mm^2/s; $P = 0.001$) or poorly differentiated tumors (1.03 ± 0.1 vs. $0.86 \pm 0.0 \times 10^{-3}$ mm^2/s; $P = 0.043$), but not in the well-

TABLE 5. Diagnostic Results in Determining Tumor Origins from Cervix or Endometrium[a]

	n	TP	TN	FP	FN	Sensitivity	Specificity	Accuracy	PPV	NPV
Training dataset										
Morphology	43	9	29	3	2	81.8 (48.2-97.7)	90.6 (75.0-98.0)[b]	88.4 (74.9-96.1)[b]	75.0 (42.8-94.5)	93.5 (78.6-99.2)
ADC value	43	7	25	7	4	63.6 (30.8-89.1)	78.1 (60.0-90.7)[b]	74.4 (58.8-86.5)[b]	50.0 (23.0-77.0)	86.2 (68.3-96.1)
Spectroscopy	43	8	27	5	3	72.7 (39.0-94.0)	84.4 (67.2-94.7)[b]	81.4 (66.6-91.6)[b]	61.5 (31.6-86.1)	90.0 (73.5-97.9)
MDS score[c]	43	9	31	1	2	81.8 (48.2-97.7)	96.9 (83.8-99.9)	93.0 (80.9-98.5)	90.0 (55.5-99.7)	93.9 (79.8-99.3)
Validation dataset										
Morphology	44	11	24	6	3	78.6 (49.2-95.3)	80.0 (61.4-92.3)	79.5 (64.7-90.2)[b]	64.7 (38.3-85.8)	88.9 (70.8-97.6)
ADC value	44	11	19	11	3	78.6 (49.2-95.3)	63.3 (43.9-80.1)[b]	68.2 (52.4-81.4)[b]	50.0 (28.2-71.8)	86.4 (65.1-97.1)
Spectroscopy	44	8	22	8	6	57.1 (28.9-82.3)[b]	73.3 (54.1-87.7)	68.2 (52.4-81.4)[b]	50.0 (24.7-75.3)	78.6 (59.0-91.7)
MDS score[c]	44	12	25	5	2	85.7 (57.2-98.2)	83.3 (65.3-94.4)	84.1 (69.9-93.4)	70.6 (44.0-89.7)	92.6 (75.7-99.1)

[a]Data are numbers. In parentheses are 95% confidence intervals.
ADC = apparent diffusion coefficient; TP = true positive; TN = true negative; FP = false positive; FN = false negative; PPV = positive predictive value; NPV = negative predictive value.
[b]Statistically significant by McNemar test.
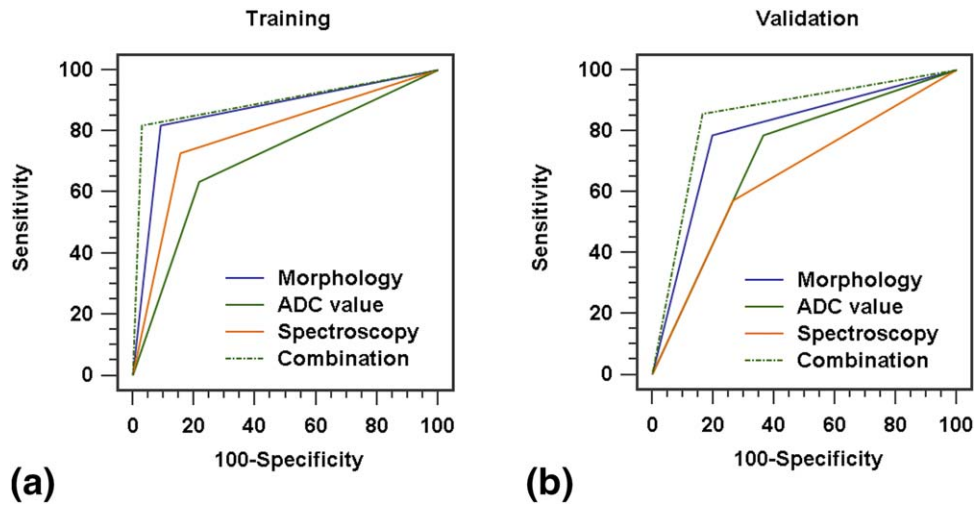[c]MDS score = combined morphology, ADC value and spectroscopy.

FIGURE 4: Comparisons of ROC curves based on morphology, ADC value, MR spectroscopy, and combinations for the training (a) and validation (b) sets.

differentiated tumors (1.05 ± 0.1 vs. $0.97 \pm 0.0 \times 10^{-3}$ mm^2/s; $P = 0.325$) (Fig. 5). The methylene $\delta 1.3$ ppm resonance was higher in cervical than in endometrial cancers for the well-differentiated (1973.5 ± 1087.5 vs. 403.0 ± 257.7 mM; $P = 0.446$), moderately differentiated (1150.0 ± 704.0 vs. 71.1 ± 23.4 mM; $P = 0.068$), or poorly differentiated tumors (2066.1 ± 1364.9 vs. 319.6 ± 134.6 mM; $P = 0.079$), albeit not statistically significant.

Discussion

Our study showed incremental values of combining quantitative DW MR imaging and MR spectroscopy to the conventional morphological MR imaging, i.e., the MDS score, in determining the origins of adenocarcinomas or adenosquamous carcinomas from cervix or endometrium. The MDS score and the cutoff values of all the parameters (ADC

values and spectroscopy) were developed based on the Training dataset, hence the performance inadvertently being robust. In the independent Validation dataset, the MDS score achieved a significantly higher accuracy than that of morphology, ADC value or spectroscopy. The clinical implication of the MDS score based on MR imaging and spectroscopy could serve as a triage test to assist clinical decision-making on choosing primary CCRT for cervical carcinomas or primary surgery for endometrial carcinomas.[3]

Bourgioti et al developed a pilot testing of an MR imaging scoring system by seven morphological characteristics for predicting tumor origin of uterine carcinomas of indeterminate histology.[18] We selected the tumor location, rim enhancement and disrupted cervical stromal integrity as three outstanding morphological traits from our training dataset. The importance of tumor location was supported

TABLE 6. Pairwise Comparisons of ROC Curves in Determining Tumor Origins from Cervix or Endometrium

	AUC	Sensitivity	Specificity	P-Value
Training dataset				
Model 1: Morphology	0.89	81.82	90.62	Reference
Model 2: Morphology and spectroscopy	0.91	90.91	81.25	0.245
Model 3: Morphology and ADC value	0.93	72.73	96.87	0.320
Model 4: MDS score[a]	0.95	81.82	96.87	0.046*
Validation dataset				
Model 1: Morphology	0.85	78.57	80.00	Reference
Model 2: Morphology and spectroscopy	0.87	85.71	80.00	0.481
Model 3: Morphology and ADC value	0.89	78.57	86.67	0.198
Model 4: MDS score†	0.90	85.71	83.33	0.289

[a]MDS score = combined morphology; ADC value and spectroscopy.
[b]Statistically significant.
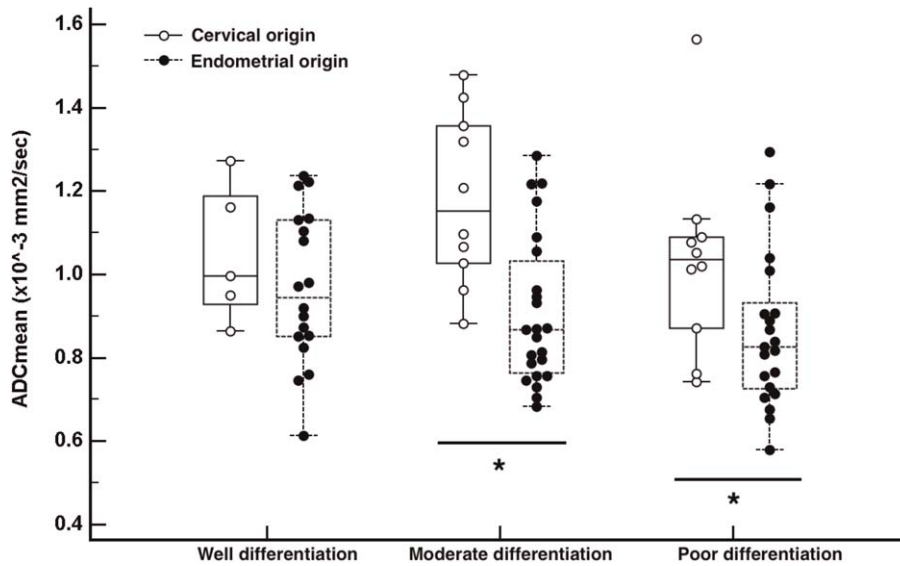ADC = apparent diffusion coefficient.

FIGURE 5: Comparison of ADC$_{mean}$ values in different tumor differentiations. $*P < 0.05$.

by data from Vargas et al, who subjectively assessed the location, and demonstrated an overall accuracy of 85–88% in attributing the cancer origin to the cervix or endometrium by using MR imaging.[9] The absence of deep myometrial invasion reported by Haider et al[10] was not a significant indicator by logistic regression in this study. The intracavitary mass and retained endometrial secretions were not selected in the MDS score because of overlapping with the tumor location. Moreover, T1-weighted dynamic-enhanced sequences aid in making the diagnosis and may help in appropriate treatment planning of these patients.[8] The relative signal for cervical cancer was approximately 30% higher than that of endometrial cancer in the arterial phase, using myometrium as an internal reference.[8,18,19] The hypervascular lesion increased the likelihood of cervical cancer, albeit statistically insignificantly in this study. A plausible explanation is that the enhancement pattern of cervical cancer was variable and also depends on the size of the tumor, which reflected on the moderate interobserver agreement.

Lin et al have demonstrated the mean ADC values were significantly higher in cervical cancer than in endometrial adenocarcinoma (0.97 vs. 0.77×10^{-3} mm^2/s),[15] based on the 2D data derived from the slice where the largest tumor section located. Our study advanced the volumetric histogram analysis of tumor ADC to minimize the slice selection bias.[20] In the analysis of cervical carcinomas, ADC was significantly higher in the well/moderately differentiated tumors compared with poorly differentiated tumors, consistently supported by reports at 3T ($0.85–1.09$ vs. $0.71–0.72 \times 10^{-3}$ mm^2/s)[21,22] or 1.5T unit ($1.14–1.38$ vs. $1.03–1.20 \times 10^{-3}$ mm^2/s).[23–25] Based on the histological correlation, ADC value was found to correlate negatively with cellular density.[21] In the endometrial cancer, ADC was

significantly higher in the well/moderately differentiated tumors compared with poorly differentiated tumors at 3T (1.04 vs. 0.81×10^{-3} mm^2/s)[26] or at 1.5T ($0.92–0.93$ vs. 0.73×10^{-3} mm^2/s).[27] Our data showed that the ADC values of adeno-/adenosquamous carcinomas from cervix were significantly higher than that from the endometrium, regardless of tumor differentiations.

Levels of methyl and methylene resonances were reported to be greater in the histologically proven cervical adeno-/adenosquamous carcinomas as compared with squamous cell carcinomas.[16] The alteration of in vivo lipid resonances was supported by reports from ex vivo tissue corroboration of cervical cancer.[28,29] The level of total choline, a mixture of cell membrane phospholipid-related metabolites, i.e., free choline, phosphocholine, and glycerophosphocholine, was more prominent in endometrial cancer, plausibly due to a relatively small peak of the lipids in the spectra. In the quantitative analysis, however, the differences of choline resonances between cervical and endometrial origins did not reach the statistical significance in the present study.

Certain restrictions were encountered in this study and warrant address here. First, from a prospective consecutive cohort, we selected patients with tumors locating at the low uterine segment or cervix, and pathology review yielded adeno- or adenosquamous carcinomas for this study. We did not include rare types, i.e., serous or clear cell carcinomas. Second, volumetric ADC histogram analysis was done, but the potentials of advanced texture analysis were not fully investigated. For the ease of clinical application and compare with literature data, we chose the ADC$_{mean}$ rather than ADC$_{10}$ in this MDS score. Third, our data are based on tumor lesion size larger than 1.5 cm for the ease of single

voxel spectroscopy acquisition, to prevent that VOI not completely covering the entire tumor volume. Cervical cancer in this size can be heterogeneous. Nonetheless, care was taken to select high signal intensity tumor area on high-*b*-value DW and low ADC, as compared with the adjacent normal cervical stroma, to minimize the VOI selection bias.

Additionally, the time and cost-effectiveness were not evaluated in this study, as MR spectroscopy as applied in the present study takes an extra acquisition time and expertise for post processing, whereas DW MR imaging is fast and easy to implement. Finally, buscopan or glucagon administrated in some other institutions to minimize the effects of bowel motion was not planned in this study. Despite these, our data demonstrated the potentials of DW MR imaging and MR spectroscopy on diagnostic accuracy of origins of cervical or endometrial cancers.

In summary, we developed and validated an MDS score based on integrated morphological, volumetric DW MR imaging and spectroscopy which has potentials to improve distinguishing adenocarcinomas of cervical or endometrial origin, and warrants large-scale studies for further validation.

Acknowledgement

References

1. Siegel RL, Miller KD, Jemal A. Cancer statistics, 2017. CA Cancer J Clin 2017;67:7–30.

2. NCCN Clinical Practice Guidelines in Oncology: Uterine Cancers. National Comprehensive Cancer Network Web site. http://www.nccn.org/professionals/physician_gls/pdf/uterine.pdf. Accessed August 22, 2017.

3. American College of O, Gynecologists. ACOG practice bulletin, clinical management guidelines for obstetrician-gynecologists, number 65, August 2005: management of endometrial cancer. Obstet Gynecol 2005;106:413–425.

4. Liao CL, Lee MY, Tyan YS, et al. Progesterone receptor does not improve the performance and test effectiveness of the conventional 3-marker panel, consisting of estrogen receptor, vimentin and carcinoembryonic antigen in distinguishing between primary endocervical and endometrial adenocarcinomas in a tissue microarray extension study. J Transl Med 2009;7:37.

5. McCluggage WG, Sumathi VP, McBride HA, Patterson A. A panel of immunohistochemical stains, including carcinoembryonic antigen, vimentin, and estrogen receptor, aids the distinction between primary endometrial and endocervical adenocarcinomas. Int J Gynecol Pathol 2002;21:11–15.

6. McCluggage WG, Jenkins D. p16 immunoreactivity may assist in the distinction between endometrial and endocervical adenocarcinoma. Int J Gynecol Pathol 2003;22:231–235.

7. Sala E, Rockall AG, Freeman SJ, Mitchell DG, Reinhold C. The added role of MR imaging in treatment stratification of patients with gynecologic malignancies: what the radiologist needs to know. Radiology 2013;266:717–740.

8. He H, Bhosale P, Wei W, Ramalingam P, Iyer R. MRI is highly specific in determining primary cervical versus endometrial cancer when biopsy results are inconclusive. Clin Radiol 2013;68:1107–1113.

9. Vargas HA, Akin O, Zheng J, et al. The value of MR imaging when the site of uterine cancer origin is uncertain. Radiology 2011;258:785–792.

10. Haider MA, Patlas M, Jhaveri K, Chapman W, Fyles A, Rosen B. Adenocarcinoma involving the uterine cervix: magnetic resonance imaging findings in tumours of endometrial, compared with cervical, origin. Can Assoc Radiol J 2006;57:43–48.

11. Ramirez PT, Frumovitz M, Milam MR, et al. Limited utility of magnetic resonance imaging in determining the primary site of disease in patients with inconclusive endometrial biopsy. Int J Gynecol Cancer 2010;20:1344–1349.

12. Lin G, Ng KK, Chang CJ, et al. Myometrial invasion in endometrial cancer: diagnostic accuracy of diffusion-weighted 3.0-T MR imaging--initial experience. Radiology 2009;250:784–792.

13. Beddy P, Moyle P, Kataoka M, et al. Evaluation of depth of myometrial invasion and overall staging in endometrial cancer: comparison of diffusion-weighted and dynamic contrast-enhanced MR imaging. Radiology 2012;262:530–537.

14. Lin G, Huang YT, Chao A, et al. Endometrial cancer with cervical stromal invasion: diagnostic accuracy of diffusion-weighted and dynamic contrast enhanced MR imaging at 3T. Eur Radiol 2017;27:1867–1876.

15. Lin YC, Lin G, Chen YR, Yen TC, Wang CC, Ng KK. Role of magnetic resonance imaging and apparent diffusion coefficient at 3T in distinguishing between adenocarcinoma of the uterine cervix and endometrium. Chang Gung Med J 2011;34:93–100.

16. Lin G, Lai CH, Tsai SY, et al. 1 H MR spectroscopy in cervical carcinoma using external phase array body coil at 3.0 Tesla: prediction of poor prognostic human papillomavirus genotypes. J Magn Reson Imaging 2017;45:899–907.

17. Collins GS, Reitsma JB, Altman DG, Moons KG. Transparent Reporting of a multivariable prediction model for Individual Prognosis Or Diagnosis (TRIPOD): the TRIPOD statement. Ann Intern Med 2015;162:55–63.

18. Bourgioti C, Chatoupis K, Panourgias E, et al. Endometrial vs. cervical cancer: development and pilot testing of a magnetic resonance imaging (MRI) scoring system for predicting tumor origin of uterine carcinomas of indeterminate histology. Abdom Imaging 2015;40:2529–2540.

19. Lin CN, Liao YS, Chen WC, Wang YS, Lee LW. Use of myometrium as an internal reference for endometrial and cervical cancer on multiphase contrast-enhanced MRI. PLoS One 2016;11:e0157820.

20. Nougaret S, Reinhold C, Alsharif SS, et al. Endometrial cancer: combined MR volumetry and diffusion-weighted imaging for assessment of myometrial and lymphovascular invasion and tumor grade. Radiology 2015;276:797–808.

21. Liu Y, Bai R, Sun H, Liu H, Wang D. Diffusion-weighted magnetic resonance imaging of uterine cervical cancer. J Comput Assist Tomogr 2009;33:858–862.

22. Kuang F, Ren J, Zhong Q, Liyuan F, Huan Y, Chen Z. The value of apparent diffusion coefficient in the assessment of cervical cancer. Eur Radiol 2013;23:1050–1058.

23. Payne GS, Schmidt M, Morgan VA, et al. Evaluation of magnetic resonance diffusion and spectroscopy measurements as predictive biomarkers in stage 1 cervical cancer. Gynecol Oncol 2010;116:246–252.

24. Xue H, Ren C, Yang J, et al. Histogram analysis of apparent diffusion coefficient for the assessment of local aggressiveness of cervical cancer. Arch Gynecol Obstet 2014;290:341–348.

25. Downey K, Riches SF, Morgan VA, et al. Relationship between imaging biomarkers of stage I cervical cancer and poor-prognosis histologic features: quantitative histogram analysis of diffusion-weighted MR images. AJR Am J Roentgenol 2013;200:314–320.

26. Lin G, Huang YT, Chao A, et al. Influence of menopausal status on diagnostic accuracy of myometrial invasion in endometrial cancer: diffusion-weighted and dynamic contrast-enhanced MRI at 3 T. Clin Radiol 2015;70:1260–1268.

27. Tamai K, Koyama T, Saga T, et al. Diffusion-weighted MR imaging of uterine endometrial cancer. J Magn Reson Imaging 2007;26: 682–687.

28. Zietkowski D, Davidson RL, Eykyn TR, De Silva SS, deSouza NM, Payne GS. Detection of cancer in cervical tissue biopsies using mobile lipid resonances measured with diffusion-weighted 1H magnetic resonance spectroscopy. NMR Biomed 2010;23:382–390.

29. Mahon MM, deSouza NM, Dina R, et al. Preinvasive and invasive cervical cancer: an ex vivo proton magic angle spinning magnetic resonance spectroscopy study. NMR Biomed 2004;17:144–153.